Cell Stem Cell
Article

Self-Organized Formation of Polarized Cortical Tissues from ESCs and Its Active Manipulation by Extrinsic Signals

Mototsugu Eiraku,[1] Kiichi Watanabe,[1] Mami Matsuo-Takasaki,[1] Masako Kawada,[1] Shigenobu Yonemura,[2] Michiru Matsumura,[1] Takafumi Wataya,[1] Ayaka Nishiyama,[1] Keiko Muguruma,[1] and Yoshiki Sasai[1,*]
[1]Organogenesis and Neurogenesis Group
[2]Electron Microscope Laboratory
RIKEN Center for Developmental Biology, Kobe 650-0047, Japan
*Correspondence: yoshikisasai@cdb.riken.jp
DOI 10.1016/j.stem.2008.09.002

SUMMARY

Here, we demonstrate self-organized formation of apico-basally polarized cortical tissues from ESCs using an efficient three-dimensional aggregation culture (SFEBq culture). The generated cortical neurons are functional, transplantable, and capable of forming proper long-range connections in vivo and in vitro. The regional identity of the generated pallial tissues can be selectively controlled (into olfactory bulb, rostral and caudal cortices, hem, and choroid plexus) by secreted patterning factors such as Fgf, Wnt, and BMP. In addition, the in vivo-mimicking birth order of distinct cortical neurons permits the selective generation of particular layer-specific neurons by timed induction of cell-cycle exit. Importantly, cortical tissues generated from mouse and human ESCs form a self-organized structure that includes four distinct zones (ventricular, early and late cortical-plate, and Cajal-Retzius cell zones) along the apico-basal direction. Thus, spatial and temporal aspects of early corticogenesis are recapitulated and can be manipulated in this ESC culture.

INTRODUCTION

During embryogenesis, the telencephalic anlage is subdivided into the Pax6$^+$ dorsal region (the pallium), which forms the cortex, cortical hem and choroid plexus, and the Pax6$^-$ ventral region (the subpallium), which forms the basal ganglia (Guillemot, 2005; Puelles et al., 2000; Rallu et al., 2002).

We recently established an efficient culture method for the selective neural differentiation of mouse ESCs (mESCs) using serum-free suspension culture (serum-free culture of embryoid body-like aggregates [SFEB]; Watanabe et al., 2005, 2007). Neural differentiation in the SFEB culture occurs tissue-autonomously and does not require extrinsic inducers (Watanabe et al., 2005). Importantly, SFEB-cultured mESCs differentiate into Bf1 (FoxG1)$^+$ telencephalic progenitors (Tao and Lai, 1992; Hanashima et al., 2004) at a moderately high frequency (Watanabe et al., 2005). The majority of the SFEB-induced telencephalic progenitors express the pallial marker Pax6, while Shh treatment suppresses Pax6 and induces the subpallial markers such as Nkx2.1 (Watanabe et al., 2005). A similar observation of telencephalic differentiation has been reported for SFEB-cultured human ESCs (hESCs) (Watanabe et al., 2007).

In this report, first, we introduce an improved three-dimensional aggregate culture that allows highly efficient differentiation of ESCs into cortical progenitors and functional projection neurons. Then, using this ESC culture, we demonstrate the in vitro recapitulation of embryonic corticogenesis and its manipulation with respect to layer-specific neurogenesis and regional specification. Finally, we demonstrate that cortical progenitors generated in this culture by mouse and human ESCs spontaneously form patterned structures, mimicking the early aspect of corticogenesis. We discuss the remarkable ability of ESC-derived cortical neuroepithelia with regard to self-organized tissue formation.

RESULTS

Efficient Differentiation of Mouse ESCs into Polarized Cortical-Type Neuroepithelia in SFEBq Culture

The previously reported SFEB method uses a suspension culture of dissociated mouse ESCs that undergo spontaneous reaggregation in 1 to 2 days. After 7 days of suspension culture, the aggregates are then subjected to adhesion culture (Watanabe et al., 2005). In this original method, the ESC aggregates form in varying sizes and the Bf1 induction efficiency is below 50% (typically, 30%–35% of total cells; Watanabe et al., 2005).

In the present study, we sought to design conditions in which the aggregate formation would be more tightly and quantitatively controlled. Dissociated mESCs (3000 cells) were cultured in each well of a low cell-adhesion 96-well plate (U-bottomed). In this procedure, the cells reaggregated quickly (within a few hours), formed uniformly sized cell masses (Figure 1A and Figure S1A available online) and selectively differentiated into neural cells (shown below). Importantly, under these conditions, a greater portion of Bf1$^+$ progenitors was reproducibly generated (up to 65%–75% of total cells on days 10 and 12; Figure 1A and also shown below) than with the original method. Moreover, the majority of the Bf1$^+$ cells (89%; day 10) generated in this modified SFEB culture coexpressed the bona fide cortical marker Emx1 (Figure 1A; in contrast, 36%–40% of Bf1$^+$ cells express

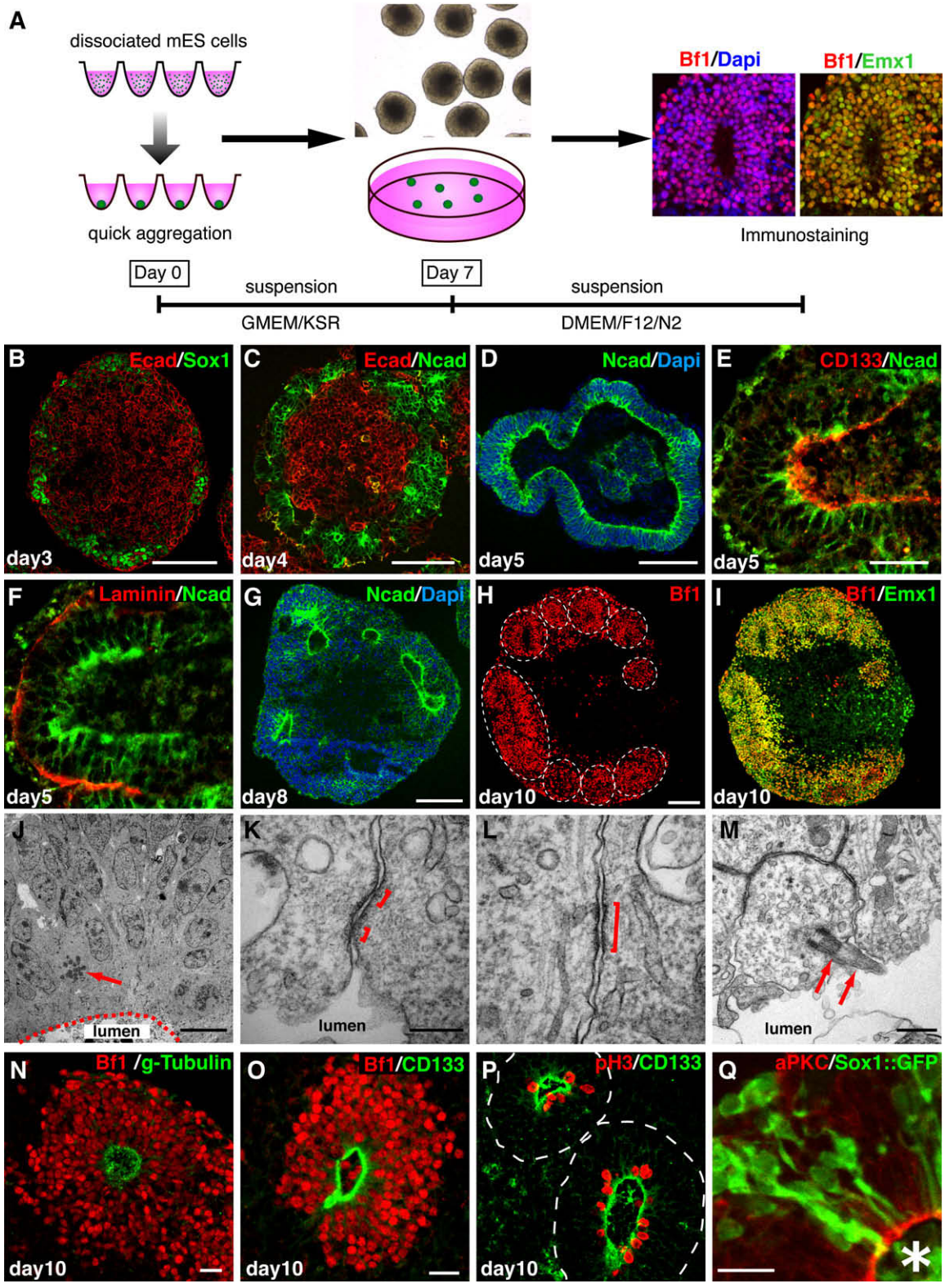

Figure 1. Generation of Polarized Cortical Neuroepithelia from SFEBq-Cultured mESCs

(A) Schematic of the SFEBq culture for mESCs. Uniformly sized aggregates on day 7 and high percentages of $Bf1^{+}/Emx1^{+}$ cells on day 10.

(B–I) Cryosections of SFEBq-cultured mESC aggregates on day 3 (B), day 4 (C), day 5 (D–F), day 8 (G), and day 10 (H and I). Immunostaining for E-cadherin (B and C), Sox1 (B), N-cadherin (D–G), CD133 (E), Laminin (F), Bf1 (H and I), and Emx1 (I).

(J–M) Electron microscopic analysis. Arrow, M-phase cell at the apical end (J) and an apical cilia (M). Bracket, tight junctions (K) and adherence junction (L).

Emx1 at most in the original SFEBq culture; Watanabe et al., 2005 and data not shown). Thus, this modified quick-aggregation procedure (SFEBq, hereafter) is much more effective for inducing the differentiation of cortical cells than is the original SFEB culture, which relies on slow reaggregation in Petri dishes.

In addition to controlling the size of the aggregates, early restoration of the cell-cell interaction by quick aggregation might also improve the selectivity and reproducibility of differentiation in this new culture procedure. In fact, one of the remarkable features of the SFEBq culture was that the ESC-derived neural progenitors reproducibly (>95%; <30% in the original SFEB culture) formed polarized neuroepithelial structures within the aggregates during the first 5 days (Figures 1B–1F). On day 3, Sox1 (earliest neuroectodermal marker) expression was first detected in the superficial zone of the SFEBq aggregate (still E-cadherin$^+$; Figure 1B), which had not yet underwent evident neuroepithelial formation. N-cadherin$^+$ neural progenitors started to accumulate in the Sox1$^+$ outer regions (gradually expanding inwards) between days 3.5 and 4 of SFEBq culture (Figure S1B). On day 4, the N-cadherin$^+$ tissues exhibited partial neuroepithelial structures (Figure 1C; see Figure S1C for a high-magnification view; the arrows indicate N-cadherin-dense apical portions while the dotted lines show the basal side). By day 5, continuous, polarized N-cadherin$^+$ neuroepithelial structures (columnar epithelia) had formed from mESC aggregates (Figure 1D; the cavitation in the SFEBq aggregate was partly due to apoptosis in a minority of cells near the center; data not shown). The aggregates reproducibly formed an apical surface inside, which was indicated by dense N-cadherin accumulation; the inner area was also positive for the apical marker CD133/Prominin1 (Weigmann et al., 1997), aPKC, and ZO-1 (Figure 1E and Figure S1D), while a basal surface (Laminin$^+$; Figure S1E for in vivo expression) was located outside (Figure 1F).

When an SFEBq aggregate was cultured in suspension beyond day 6, the continuous neuroepithelial sheet (Figure 1D) gradually reformed into several round clusters (rosettes) around days 7 and 8 (Figure 1G). The number of Bf1$^+$/Emx1$^+$ rosettes per aggregate peaked around day 10 (Figures 1H and 1I and Figures S1F–S1J). Electron microscopic analysis (Figures 1J–1M) showed the presence of tight (Figure 1K) and adherence (Figure 1L) junctions as well as apical cilia structures (Figure 1M; 9+0 tubulin arrangement in Figure S1K) on the lumenal side. Consistent with this epithelial polarity, the apical-end markers (gamma-tubulin$^+$, CD133$^+$) were localized at the center of each rosette facing to the lumen (Figures 1N and 1O). Phosphorylated histone H3 (pH3), a marker for the G2-M phases, was detected in Emx1$^+$ nuclei close to the center (Figure 1P); this distribution was reminiscent of the in vivo position of pH3$^+$ cortical neuroepithelial nuclei in the apical zone (Figure S1L). Individual neuroepithelial cells in the ESC-derived rosettes, visualized by mixing *Sox1::GFP*-knockin ESCs with nonlabeled ESCs in the reaggregation culture on day 0, showed a typical morphology of the neural progenitors in the early embryonic neuroepithelium and expressed aPKC, an apical marker, on the luminal side (Figure 1Q).

Thus, the SFEBq culture efficiently and reproducibly induces the formation of Bf1$^+$/Emx1$^+$ neuroepithelia with an evident polarity similar to the embryonic neuroepithelial structure.

SFEBq-Induced Neuroepithelia Generate Cortical-Type Neurons

In dissociation culture, the SFEBq-induced neural progenitors (dissociated on day 12) differentiated into Tuj1$^+$ postmitotic neurons expressing characteristic cortical markers such as Emx1 (82%) and VGLUT1 (83%), as well as Telencephalin (Mitsui et al., 2007), CamKIIa (Kinney et al., 2006), and GluR1 (Figure 2A and Figures S2A–S2D). They also expressed subtype-specific markers such as Tbr1, Ctip2, and Brn2 (Figures S2E–S2H and data not shown).

We then performed an organotypic coculture with embryonic forebrain tissues using ESCs with *Venus-GFP* (Nagai et al., 2002) knocked in at the *Bf1* gene locus (see Figures S2I–S2N and Supplemental Experimental Procedures). The ESC-derived Bf1::Venus$^+$ cell masses (day 14 of culture) were placed within the lateral ventricles of the forebrain slice (E14.5; frontal section slices) in contact with both the pallial and subpallial walls (Figure 2C), and these conjugates were then subjected to culture on a porous filter for an additional 3 days. A large number of Bf1::Venus$^+$ cells preferentially invaded the pallial region (89% of the conjugates, n = 28). In contrast, the Bf1::Venus$^+$ cells rarely invaded the subpallial or diencephalic region (Figures 2D and 2E; Figure 2F shows the polarized arrangement of cells migrating toward the pia). Emx1, Tbr1, Ctip2, and Brn2 were expressed in >96%, 3%, 65%, and 21% of Venus$^+$ neurons in the intermediate and mantle zones, respectively (most Tbr1$^+$ neurons remained within the SFEBq aggregate; data not shown). Efficient integration of the Bf1::Venus$^+$ neurons was also observed when the day 14 aggregates were cocultured with postnatal (P1) forebrain slices (70% of the conjugates, n = 20; Figures 2G–2I; arrowheads in Figure 2I indicate extending axons; the distribution of integrated neurons expressing subtype-specific markers is shown in Figures S2O–S2R).

We next transplanted Bf1::Venus$^+$ cells into the in vivo neonatal brain. Bf1::Venus$^+$ cells were dissociated and injected into the neonatal cortex (P2; see the Supplemental Experimental Procedures). Four weeks later, a number of Bf1::Venus$^+$ pyramidal neuron-like cells with a well-developed apical dendrite and several basal dendrites were observed (Figures 2J–2L; 71% of Venus$^+$ cells). When Bf1::Venus$^+$ cell aggregates were grafted en bloc into the frontal cortex (Figures 2M–2O and Figure S2S), numerous Venus$^+$ axons were observed in the deep cortex zone, corpus callosum, striatum (observed as fascicles), thalamus, cerebral peduncle (pyramidal tract), and pontine nuclear regions, consistent with the corticofugal axons projecting from the embryonic cortical neurons (Figures 2P–2U). In addition, an overlay study on P1 slices showed that the Venus$^+$ axons from the SFEBq aggregates actively turned their directions toward the subcerebral regions and away from the cortex (Figures S2T–S2W).

These findings supported the idea that the SFEBq-induced Bf1$^+$ progenitors can function as bona fide progenitors for cortical projection neurons.

(N–Q) Immunostaining of rosettes in the SFEBq aggregates for Bf1 (N and O), gamma-tubulin (N), CD133 (O and P), phosphorylated H3 (P), and aPKC ([Q]; asterisk, lumen). In (Q), *Sox1::GFP* ESCs were mixed with nonlabeled ESCs upon reaggregation on day 0.
Scale bars: 100 μm in (B)–(D), (G), and (H); 50 μm in (E) and (F); 10 μm in (J); 0.2 μm in (K) and (L); 0.5 μm in (M); and 20 μm in (N)–(Q).

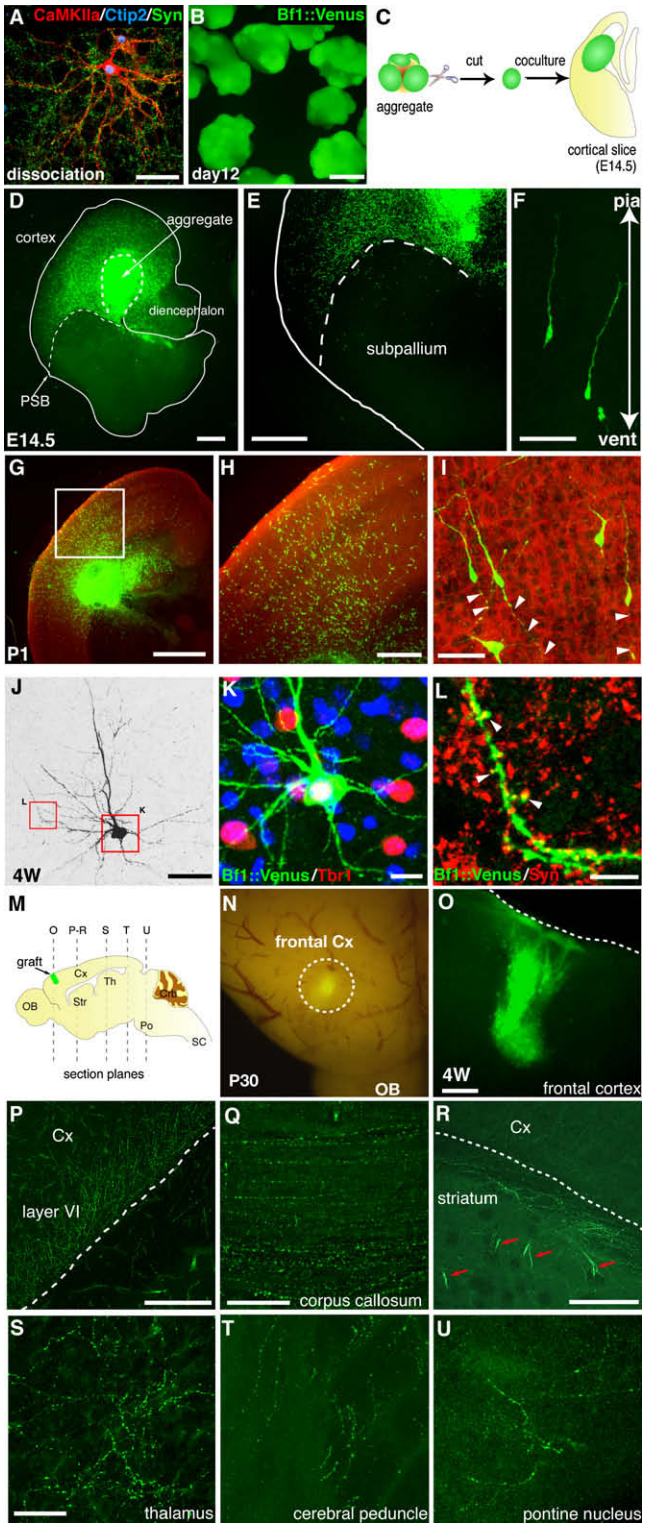

Figure 2. Intergration of SFEBq-Induced Cortical Neurons with Cortical Tissues

(A) An example of Ctip2$^+$ stellate-shaped neurons receiving numerous Synaptophysin$^+$ presynaptic inputs on the well-arborized CamKII$^+$ dendrites in long-term dissociation culture, day 42.

(B) SFEBq-cultured mESC aggregates (*Bf1::Venus*) on day 12.

(C) Schematic of the coculture study using forebrain slices (E14.5).

(D and E) Invasion of Venus$^+$ neurons into the cortical region of the E14.5 slice.

(F) A high magnification view of migrating Venus$^+$ neurons.

(G–I) Invasion of Venus$^+$ neurons into the cortical region of the P1 slice. Immunostaining for Venus (anti-GFP, green) and L1 (red). (I) High magnification confocal image. Arrows, extending axons.

(J–L) An example of typical pyramidal neurons generated from the SFEBq-derived cortical progenitors (day 14) dissociated and injected into the P2 neocortex 4 weeks after grafting. (J) Negative image of GFP expression. (K) Immunostaining for Bf1::Venus-GFP and Tbr1. (L) Immunostaining for Bf1::Venus-GFP and synaptophysin.

(M–U) Bf1::Venus$^+$ cell aggregates were grafted *en bloc* into the frontal cortex. (M) Schematic of coronal sections. (N and O) The graft in the frontal cortex. (P–U) Distributions of the graft-derived Venus$^+$ axons in the boundary between the cortex (Cx) and white matter (P), the corpus callosum (Q), the striatum (R), the thalamus (S), the cerebral peduncle (T), and the pontine nucleus (U).

Scale bars: 50 μm in (A), (F), and (I); 500 μm in (B), (D), (E), and (M); 1 mm in (G); 60 μm in (J); 20 μm in (K) and (L); 300 μm in (O)–(R); and 100 μm in (S)–(U).

SFEBq-Induced Neurons, such as Neonatal Cortical Neurons, Show Spontaneous Ca^{2+} Oscillations that Expand over Long Distances

We next performed Ca^{2+} imaging studies (Ikegaya et al., 2005) using long-term cultured SFEBq-treated mESC aggregates (*Bf1::Venus*) (Figure 3A). On day 21, individual Venus$^+$ neurons showed patterned spontaneous activity that differed from neuron to neuron in frequency, regularity, and duration (Figures 3B and 3C; see Movie S1 for time-lapse image). Regardless of the patterns, this spontaneous neuronal activity (Ca^{2+} surges) increased in frequency following glutamate application (Figure 3D) and was inhibited by TTX (tetrodotoxin; Figures 3E and 3F), indicating that it was dependent on a local synaptic connection.

Previous studies have reported locally coupled spontaneous neuronal activity that is unique to the neonatal cortex during the first postnatal week: a large-scale, very fast oscillatory Ca^{2+} wave that synchronously activates neurons over a long distance (one to several millimeters; Garaschuk et al., 2000; Adelsberger et al., 2005). To our surprise, such locally-coupled Ca^{2+} transients were also reproducibly observed in the ESC-derived Bf1::Venus$^+$ tissues. The fast-wave Ca^{2+} oscillation was seen almost simultaneously over a large area (up to about 1 mm in the long axis; >1.3 mm/sec) in the aggregate (Figures 3G–3I; Figures S3A and S3B for 60 point simultaneous recording; Movies S2 and S3 for time-lapse images of this and another view field). As seen in the neonatal cortex (Garaschuk et al., 2000; Adelsberger et al., 2005), this oscillation was blocked by CNQX (a glutamate antagonist; Figure 3J) or TTX, but not by bicuculline (a GABA antagonist; data not shown). The large-scale, fast-wave Ca^{2+} oscillations were observed more frequently on day 24 in culture than on day 21 ($p < 0.01$, Student's t test; Figure 3K), probably reflecting the maturation of neuronal networks over a large area in the aggregate). A similar long-range (>1 mm) coupling of neuronal activity was observed by MED64 multigrid electrode analysis (field potential; data not shown). In addition to these long-range oscillations, short-range, slow-wave Ca^{2+} oscillations (Yuste et al., 1995) were also frequently observed (Figure S3C and Movie S4).

These findings show that the SFEBq-induced cortical tissues, at least in part, mimic neuronal activity features characteristic of neonatal cortical tissues.

Manipulation of the Regional Identity of ESC-Derived Cortical and Noncortical Pallial Tissues

These results led us to ascertain that the SFEBq-induced progenitors had the ability to produce cortical neurons. We then sought to modify the regional and temporal identities of the induced cortical tissues by manipulating the extrinsic conditions (Figures 4 and 5).

The pallium is patterned in a region-specific fashion during embryogenesis (O'Leary et al., 2007). The rostral-most part of the cortex is the olfactory bulb, which is an extension of the medial pallium. The cortical hem and choroid plexus arise from the caudal-dorsal end of the pallium (Monuki and Walsh, 2001). The neocortex is located between these areas and itself is patterned along the rostral-caudal axis by the rostral-low, caudal-high gradient of the transcription factor COUP-TF1 (Figure 4A and Figure S4A, left; O'Leary et al., 2007; Zhou et al., 2001). Immunostaining revealed that 47% of the SFEBq-induced Bf1:Venus$^+$ cells (sorted by FACS on day 7 and subjected to further reaggregation culture for 3 days; Figure 4B) were strongly positive for COUP-TF1 (Figures 4C and 4F), suggesting that the induced cortical cells represent heterogeneous regional identities along the rostral-caudal axis.

Fgf8 has been shown to function as an inducer of rostral cortical regions (Hebert et al., 2003b; Shimogori and Grove, 2005). Interestingly, the treatment of Bf1::Venus$^+$ cell aggregates with Fgf8 (day 7) strongly suppressed COUP-TF1 expression (12% of total cells; Figures 4D and 4F and Figure S4B). In contrast, COUP-TF1$^+$ cells were substantially increased in number by treating the aggregates with the Fgf inhibitor FGFR3-Fc (81% of of total cells; Figures 4E and 4F). These COUP-TF1$^+$ cells coexpressed the cortical marker Emx1 (Figure S4C), indicating that the FGF signal attenuation induced a caudal cortical fate. Treatment with Fgf8 or FGFR3-Fc largely did not affect the Bf1::Venus expression in the aggregates on day 10 (Figures 4G–4I).

These findings showed that Fgf signaling induces rostralization of early cortical tissues in vitro, as it does in vivo. Consistent with this idea, Tbx21/Reelin/Tbr1 coexpression, which is characteristic of the projection neurons in the olfactory bulb (Yoshihara et al., 2005), a derivative of the rostral-most cortex (Figures 4J and 4K), was induced by Fgf8 (100% of Fgf8-treated aggregates and 0% of untreated controls; Figures 4L–4N; day 21; see the Experimental Procedures).

The in vivo development of the cortical hem and choroid plexus requires Wnt and BMP signals (Lee et al., 2000; Hebert et al., 2003a). During midcorticogenesis, pallial Otx2 expression is found exclusively in the proximity of the hem (TTR$^-$) and in the choroid plexus (TTR$^+$) (Figure 4O). Treatment of Bf1::Venus$^+$ cell aggregates with Wnt3a promoted the generation of Otx2$^+$/TTR$^-$ hem-type cells (Figures 4P and 4Q). These Otx2$^+$ cells coexpressed another hem/choroid-plexus marker, Lmx1a (Mangale et al., 2008) (Figure 4R and Figure S4D), while Lmx1a was not efficiently induced by FGFR3-Fc (Figure S4E). In contrast, BMP4 treatment induced Otx2$^+$/TTR$^+$ choroid-plexus-like epithelial cells in addition to Otx2$^+$/TTR$^-$ cells, and this induction was further enhanced when Wnt3a and BMP4 treatments were combined (Figures 4S–4U and Figure S4F).

Collectively, these findings demonstrate that SFEBq culture enables considerable in vitro control of regional pallial (cortical and noncortical) tissue induction from ES-derived progenitors by the manipulation of these embryologically relevant patterning signals (Figure S4A).

Temporal Control of the Generation of Layer-Specific Cortical Neurons and their Enrichment by In Vitro Cellular Manipulation

The neocortex consists of six distinct layers, and the embryonic cortical neuroepithelia generate layer-specific neurons by the progressive commitments of cortical stem cell populations (Hevner et al., 2003a; Shen et al., 2006). During corticogenesis, the neurons of layers II–VI are born sequentially in an "inside early, outside late" order (inside-out pattern), with the exception of the Reelin$^+$/Bf1$^-$ Cajal-Retzius cells in layer I (Soriano and Del Rio, 2005; Stoykova et al., 2003), which are born the earliest (at around E10 in mice). Cajal-Retzius cells are derived from the peripheral regions of the pallium such as the Bf1$^-$ hem or Bf1$^+$ pallial-subpallial boundary regions (the hem anlage is also initially Bf1$^+$) and migrate into the superficial-most cortical zone (Bielle et al., 2005; Frantz and McConnell, 1996; Hevner et al., 2003b; Hanashima et al., 2004; Molyneaux et al., 2007). Then, precursors of the layer VI neurons (later demarcated by Tbr1$^+$/Bf1$^+$) and layer V neurons (Ctip2$^+$ /Emx1$^+$) are sequentially born and form the early cortical plate (CP), which later becomes the lower CP (Figure S5A; Hevner et al., 2001; Arlotta et al., 2005). During late corticogenesis, the late/upper CP neurons and their progenitors, occupying the VZ/SVZ during mid-late gestation, express Brn2 (Figure S5B; Hevner et al., 2003a; Frantz and McConnell, 1996; Molyneaux et al., 2007).

As illustrated in Figure 5A, the sequence of marker expression onset in the SFEBq culture generally paralleled that seen during embryogenesis. Reelin$^+$ and Tbr1$^+$/Reelin$^-$/Bf1$^+$ neurons appeared on days 7 and 8, while substantial numbers of Ctip2$^+$/Emx1$^+$ neurons were seen only on and after day 10 (Figure 5B). Brn2$^+$/Bf1$^+$ cells showed substantially increased numbers during days 10–13 (Figure 5C; initially mitotic), and most became postmitotic (TuJ1$^+$) by day 15 (Figure 5D) These Brn2$^+$ neurons also expressed other upper CP markers such as Cux1 and Satb2 (Figures S5C and S5D and data not shown).

For a birth-date analysis (Ajioka and Nakajima, 2005; Gonzalez et al., 1997), the SFEBq-induced neural progenitors were incubated overnight with BrdU during days 8–14 in culture, and the BrdU-labeled cells were analyzed with neuron-type-specific markers on day 16 (Figures 5E–5I). We found that the birth (the timing of the last S phase) of Reelin$^+$ (layer I), Tbr1$^+$/Bf1$^+$ (layer VI), Ctip2$^+$ /Emx1$^+$ (layer V), and Brn2$^+$/Tuj1$^+$ (layer II/III) neurons peaked on days 8–10, 9 to 10, 10 to 11, and 12 to 13, respectively (Figure 5I), showing that the layer-specific neurons from mESC-derived cortical progenitors were preferentially generated in the same temporal order as seen in the embryonic mouse cortex (Gonzalez et al., 1997). These observations are in accordance with the intrinsic temporal program of cortical neurogenesis shown with cortical progenitors derived from the embryonic brain (Shen et al., 2006) and, very recently, with those from ESCs (Gaspard et al., 2008).

Based on these findings, we next asked whether very early-born Reelin$^+$ neurons and early CP neurons (Ctip2$^+$), respectively, could be preferentially generated by the timed control of neuronal induction in SFEBq culture. *Bf1::Venus* ESCs were

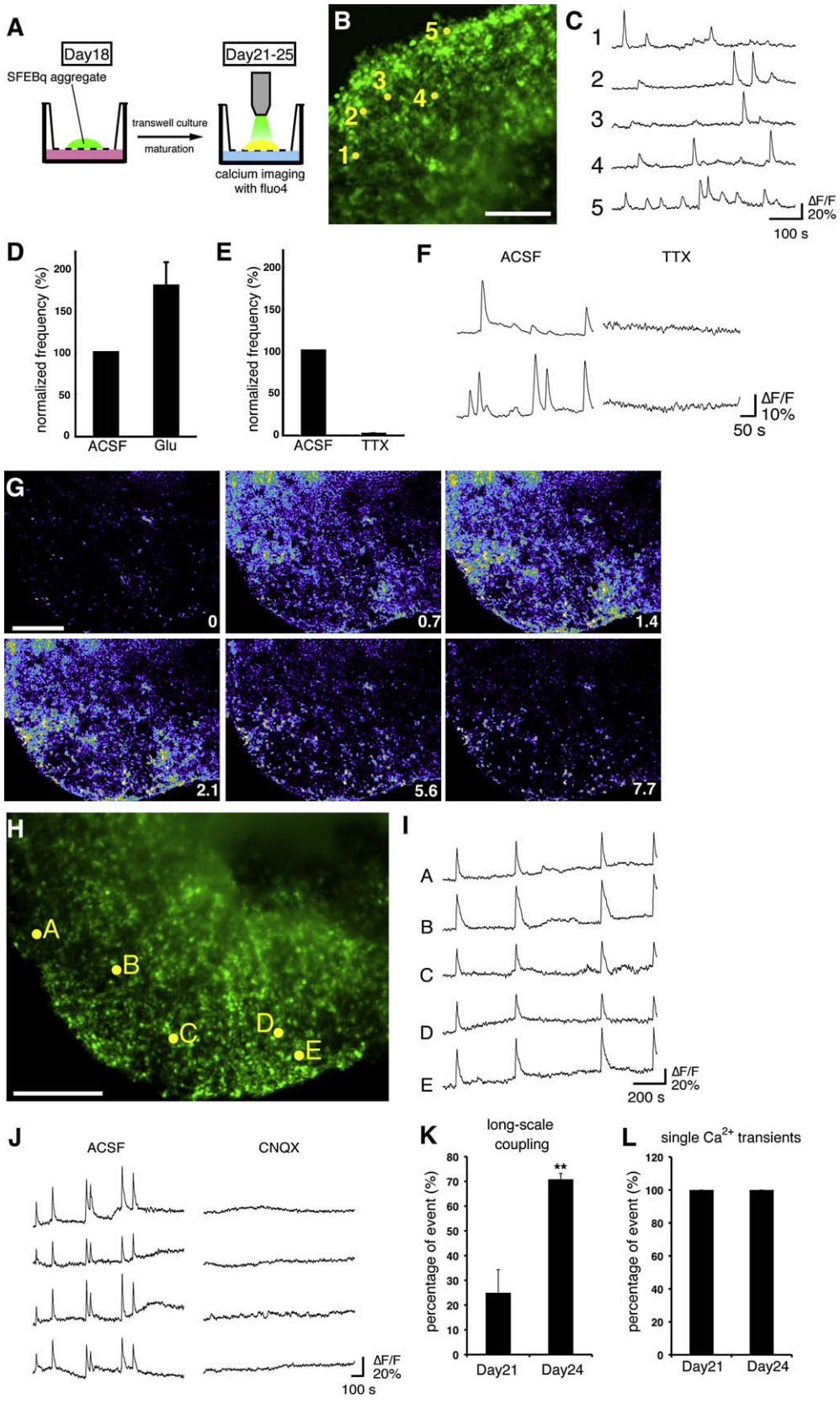
A
Day18
SFEBq aggregate
transwell culture
maturation
Day21-25
calcium imaging
with fluo4
B
C
ΔF/F
20%
100 s
D
normalized frequency (%)
ACSF
Glu
E
ACSF
TTX
F
ACSF
TTX
ΔF/F
10%
50 s
G
0
0.7
1.4
2.1
5.6
7.7
H
A
B
C
D
E
I
ΔF/F
20%
200 s
J
ACSF
CNQX
ΔF/F
20%
100 s
K
long-scale
coupling
percentage of event (%)
Day21
Day24
L
single Ca2+ transients
percentage of event (%)
Day21
Day24

cultured by SFEBq for different times, at which point the Venus$^+$ cells were sorted by FACS and quickly reaggregated, followed by suspension culture in the presence of the Notch inhibitor DAPT, which promotes neuronal differentiation from mitotic progenitors (Nelson et al., 2007; Figure 5J and Figures S1P and S1Q). Reelin$^+$ cells were predominant when the Bf1::Venus$^+$ cells were sorted on day 9 and treated with DAPI (Figures 5K and 5N). In contrast, the majority of cells became Ctip2$^+$ (strongly positive in 66% of the cells) when the Bf1::Venus$^+$ cells were induced to differentiate into neurons on day 12 and cultured for another 7 days (Figures 5L and 5O; cortical neuronal differentiation occurred slightly more slowly in the *Bf1::Venus* ESCs and Ctip2 expression appeared about 0.5 to 1 day later than in the wild-type ESCs that were used in Figure 5I; data not shown). The Ctip2$^+$ cells coexpressed Emx1 (Figure 5M) and GAD$^-$ (Figure S5E), indicating that these cells represented early CP neurons. In contrast, the percentage of Reelin$^+$ cells was low (7%; Figure 5N) after this late-step induction (5% without DAPT treatment; Figure S5F). Only a marginal increase in Brn2$^+$ neurons was observed by neuronal induction on day 12 as compared to the Brn2$^+$ proportion after the day 9 induction (Figure 5P).

Thus, SFEBq culture not only recapitulates the temporal aspects of cortical neurogenesis, but also is applicable to selective generation of layer-specific neurons in vitro (Figure S5H).

Generation of Cajal-Retzius Cells and Cortical-Plate Neurons from Polarized Cortical Neuroepithelial Tissues in SFEBq Culture

We next examined how such cell-type-specific differentiation occurred in the structural context of the SFEBq aggregate.

On day 7, about a half of the Reelin$^+$ cells were found in Bf1$^-$ cell masses located adjacent to, and often continuous with, Bf1$^+$ rosettes (Figure 6A), while the Bf1$^+$ rosettes also contained Reelin$^+$ cells, most of which were weakly positive (Figure 6A and Figure S6A). On day 8, the majority of Reelin$^+$ cells were clearly Bf1$^-$, only loosely clustered and located mainly outside of the Bf1$^+$ rosettes (Figure 6B and Figures S6B and S6C). On day 10, Reelin$^+$/Tbr1$^+$ neurons, which represented ~15% of the total cells and coexpressed another Cajal-Retzius cell marker Calretinin (Figures S6E–S6H; Englund et al., 2005; Hevner et al., 2003b; Soriano and Del Rio, 2005; Stoykova et al., 2003), were found in the nonrosette regions and the thin superficial-most zones of the Emx1$^+$ cortical rosettes (Figure 6C).

On day 10, each SFEBq-cultured ESC aggregate contained several Emx1$^+$ rosettes that had Pax6$^+$ areas in the central zones (Figure 6D). These inner portions (Bf1$^+$/Pax6$^+$) were occupied by mitotic (Ki67$^+$) neuroepithelial cells (Figure S6I). In the Bf1$^+$ region, the rosettes were circumferentially surrounded by neurons that were Emx1$^+$, Tbr1$^+$, Pax6$^-$, and Reelin$^-$ (Figures 6C and 6D and data not shown); this marker expression profile is characteristic of the early/lower CP neurons during early in vivo corticogenesis (Figure S6K; Englund et al., 2005; Hevner et al., 2001).

Tbr2 is a marker for the progenitors and precursors of late/upper CP neurons (Englund et al., 2005; Hevner et al., 2001). Prior to the formation of the late/upper CP in the embryonic cortex, Tbr2$^+$ late CP precursors are mostly mitotic (Ki67$^+$ and Pax6$^+$) and occupy the cortical subventricular zone (Figure S6J; Englund et al., 2005). In the SFEBq culture, Tbr2 appeared later (days 9 and 10) than the early CP marker Tbr1 (days 7 and 8; Figure 5A). On day 10, in contrast to the postmitotic Tbr1$^+$ cells surrounding the rosette, most of the Tbr2$^+$ cells were found particularly in the outer portion of the Pax6$^+$ zone (or adjacent part of the Tbr1$^+$ regions; Figures 6E). This distribution pattern of Tbr2$^+$ cells in the Pax6$^+$ zone is reminiscent of the in vivo situation (subventricular location; Figure 6F and Figures S6J and S6K).

After day 12 in SFEBq culture, polarized rosette structures gradually began to disintegrate as the neuroepithelial progenitors (i.e., the radial glia of cortical tissues) decreased in number. Most of the Pax6$^+$ neuroepithelial progenitors disappeared and underwent neuronal differentiation by day 16 (Figure 5D and Figure S1O). Unlike in the embryonic neocortex, the "inside-out pattern" of layer-specific neurons was not observed, even at this late phase of SFEBq culture. For instance, double staining for the early CP (Ctip2) and late CP (Satb2, Brn2) markers on day 16 showed that the early and late CP markers were mostly found in the outer and inner portions of the cortical cell clusters, respectively, suggesting that the layer inversion (early, deep; late, superficial) did not occur (Figures 6G–6I, and data not shown); the situation was similar on day 19 (Figures S6L–S6O).

Taken together, these findings indicate that SFEBq-induced cortical rosettes have the apico-basal arrangement of four distinct zones (Pax6$^+$, Tbr2$^+$, Tbr1$^+$, and Reelin$^+$), mimicking structural aspects of the early cortical tissue prior to the upper/late CP formation.

Application of SFEBq Culture to hESC Differentiation

Lastly, we tested whether the SFEBq culture procedure is applicable to the formation of polarized cortical neuroepithelial tissues in human embryonic stem cell (hESC) culture. In this case, ROCK inhibitor treatment (see Experimental Procedures and Figure S7A) was essential for circumventing the hESC-specific apoptosis that is induced by cellular dissociation and suspension (Watanabe et al., 2007). Like the mESCs, the SFEBq-cultured hESCs formed N-cadherin$^+$/BLBP$^+$ neuroepithelia that

Figure 3. Spontaneous Ca^{2+} Oscillations in mESC-Derived Cortical Tissues

(A) Schematic of Ca^{2+} imaging. The Venus signals were much weaker than Fluo4 signals and, therefore, negligible in this image.

(B and C) Analysis of Ca^{2+} surges in individual neurons on day 21. Numbers correspond to individual neurons analyzed simultaneously by Ca^{2+} imaging. (B) Fluo4 fluorescence image at the peak signal point.

(D–F) Effects of glutamate (100 μM) (D) and TTX (1 μM) (E and F) on Ca^{2+} surges in individual neurons. ACSF, artificial CSF.

(G–I) Long-scale synchronous Ca^{2+} oscillations on day 24. (G) Pseudocolor images after baseline signal subtraction. (H and I) Neurons A–E correspond to individual cells analyzed simultaneously by Ca^{2+} imaging.

(J) Effects of CNQX (10 μM) on large-scale Ca^{2+} coupling.

(K and L) Comparison of percentages of aggregates showing long-range Ca^{2+} oscillations between days 21 and 24 (K). $^{**}p < 0.01$, t test. In contrast, no significant difference was seen for the appearance of single Ca^{2+} transients in the aggregates (L).

Scale bars: 100 μm in (B) and 200 μm in (G) and (H). The bars in the graphs represent standard errors.

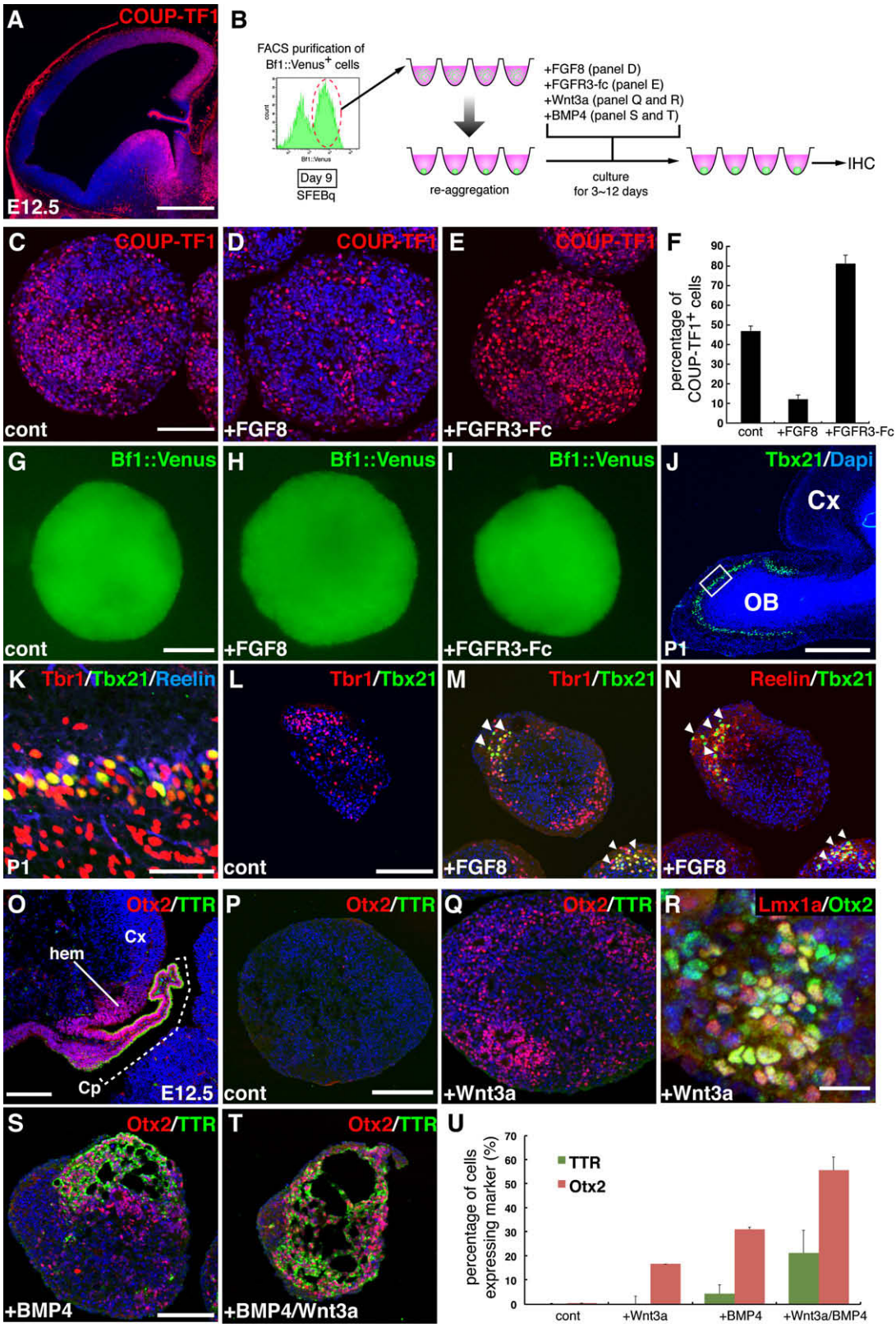

Figure 4. Active Manipulation of the Regional Specification in the SFEBq-Induced Cortical Progenitors by the Extrinsic Conditions

(A) Immunostaining of COUP-TF1 in the E12.5 mouse cortex (parasagittal section; rostral, left).

(B) Schematic of the experiments of the patterning factor treatments.

were highly polarized (>95% aggregates; Figures 6J–6L and Figure S7B) and expressed Bf1, Emx1, and Pax6 (Figures 6M and 6N). Interestingly, unlike the mESC-derived tissues, the hESC-derived Bf1$^+$/Emx1$^+$/Pax6$^+$ neuroepithelium did not reform into many small rosettes but instead formed one or a few relatively large torus-like or mushroom-shaped structures even after 46 days in differentiation culture (Figures 6J–6N; found in >90% of the aggregates).

On day 46, Tbr1$^+$ neurons were mainly found in the TuJ1$^+$ zones surrounding the Bf1$^+$/Pax6$^+$ neuroepithelia (Figures 6N–6P). In the hESC-derived cortical neuroepithelial domain, the superficial-most layer of the Tbr1$^+$ zone contained Reelin$^+$/Tbr1$^+$/Bf1$^-$ Cajal-Retzius-like cells (Figure 6O and Figure S7C). The Bf1$^+$/TuJ1$^+$ postmitotic neurons in the outer zone also expressed another early CP marker Ctip2 (Figures 6Q). In contrast, the late CP marker Tbr2 was mostly seen within the Pax6$^+$ ventricular zone-like region on day 46, particularly near the boundary to the Tbr1$^+$ regions (Figures 6R). Thus, the early spatial expression patterns of these markers were consistent between the mESC- and hESC-derived cortical tissues (Figure S7D).

Later around day 60, as with the mESC-derived tissues, the continuous cortical neuroepithelia broke into several relatively large rosettes (Figure S7F and data not shown; day 59), which had the same relative distribution of cortical neurons and progenitors as seen on day 46 (Figures S7F–S7I). On day 59, however, the Pax6$^+$ progenitor zone became much thinner (typically 5–7 nucleus thickness; Figure S7G) than that on day 46 (11–14 nucleus thickness; Figure 6M) and disappeared later (e.g., day 106).

DISCUSSION

Region- and Timing-Specific Control of the Generation of Cortical/Pallial Tissues from ESC-Derived Progenitors

In this report, we have described a highly reproducible three-dimensional culture of ESCs following their quick dissociation and reaggregation and shown the efficient formation in this culture of polarized Bf1$^+$/Emx1$^+$ neuroepithelia that generate multiple kinds of cortical-type neurons in a temporally and spatially coordinated fashion. As shown in this and other studies (Watanabe et al., 2005, 2007; Gaspard et al., 2008), the telencephalic differentiation of ESCs is largely dependent on cell-intrinsic mechanisms and weak/basal endogenous extracellular signals, but not on strong inductive signals. Probably because of this feature, the telencephalic differentiation of ESCs appears to be quite sensitive to relatively minor changes in the initial culture conditions such as the cell density, aggregate formation, cell adhesion, and basal culture medium (Watanabe et al., 2005; Wataya et al., 2008).

Our SFEBq approach permits a particularly faithful recapitulation of early corticogenesis. Furthermore, several aspects of in vitro cortical differentiation are extrinsically controllable by signal manipulation in this culture. By modifying extrinsic signals, SFEB-induced Bf1::Venus$^+$ cells can be specified into a wide variety of region-specific pallial tissues (Figure 4 and Figure S4A). In the absence of exogenous Fgf8 or its antagonist, about a half of the Bf1::Venus$^+$ cells express COUP-TF1, suggesting that SFEBq culture per se induces a mixed cortical progenitor population with respect to the rostral-caudal specification. This may be due to the low but significant level of endogenous Fgf signals, since treatment with FGFR3-Fc can efficiently induce COUP-TF1$^+$ caudal cells. The present study has also demonstrated that Fgf8 is a "sufficient" factor for the olfactory bulb induction directly from Bf1$^+$ progenitors.

Importantly, SFEBq-induced Bf1::Venus$^+$ progenitors are steered to differentiate into the caudal-dorsal pallial tissues (noncortical; hem and choroid plexus) by Wnt and BMP signals. These findings demonstrate remarkable direct changeability of the fate of Bf1$^+$ cortical progenitors into noncortical pallial tissues by simple signaling manipulation during early differentiation stages in vitro.

Taking advantage of the sequential commitment of layer-specific neurons in the SFEBq culture, we have also demonstrated the preferential generation of the very early neuronal lineage (Reelin$^+$) versus the early CP lineage (Ctip2$^+$/Emx1$^+$) (Figure 5). Forced cell-cycle exit at an early time point facilitates the generation of Reelin$^+$ Cajal-Retzius-type neurons, which are born early in vivo. In this case, forced neuronal differentiation by DAPT is essential for efficient Reelin induction from FACS-sorted Bf1::Venus$^+$ cells (Figure S5F, lanes 1 and 2). Conversely, even without FACS sorting, DAPT treatment alone (day 8) could efficiently generate Reelin$^+$ cells (up to two-thirds of total cells; Figures S1R and S1S).

In contrast, neuronal induction at a later time point results in the preferential generation of Ctip2$^+$/Emx1$^+$ neurons, whose birth date in vivo is later than that of Cajal-Retzius cells. At this late point, DAPT treatment does not substantially induce Reelin$^+$ cells any more (Figure S5E, lanes 3 and 4), probably because the competence of ESC-derived cortical progenitors to generate Reelin$^+$ cells has already been reduced by then.

Self-Organized Formation of Polarized Cortical Neuroepithelia

One of the important features of the SFEBq culture is the reproducible formation of the well-polarized cortical-type neuroepithelia (Figures 1 and 6). Since dissociated ESCs have no predetermined positional information at the beginning of culture, certain self-organizing mechanisms should be involved in the

(C–F) The effects of FGF signaling on COUP-TF1 expression. (C) untreated, (D) Fgf8b treatment (50 ng/ml, days 7–10), and (E) FGFR-Fc treatment (500 ng/ml, days 7–10). (F) Quantification of the COUP-TF1$^+$ cell percentages.
(G–I) The effects of FGF signaling on the expression of Bf1::Venus.
(J–N) Induction of olfactory bulb neurons in the SFEBq-induced cortical tissues. (J and K) Tbx21 expression in the P1 mouse olfactory bulb (OB, parasagittal section). Cx, cortex. (K) Triple-staining of Tbx21, Tbr1, and Reelin in a high magnification view. (L–N) Induction of Tbx21$^+$ neurons by Fgf8.
(O–U) Induction of hem and choroid-plexus differentiation. (O) Expression of Otx2 and TTR in the mouse hem and choroid-plexus. E12.5, parasagittal section. (P–R) Induction of Otx2 (Q and R) and Lmx1a (R) by Wnt3a treatment (20 ng/ml, days 9–12). (S and T) Induction of TTR in the SFEBq-generated neural progeniors by BMP4 ([S] and [T]; 0.5 nM, days 9–12) and Wnt3a (T). (U) Quantification of the Otx2$^+$ and TTR$^+$ percentages.
Scale bars: 400 μm in (A); 100 μm in (C)–(E), (G), (O), (P), and (Q); 50 μm in (K) and (R); 200 μm in (L)–(N); and 80 μm in (S) and (T). The bars in the graphs represent standard errors.

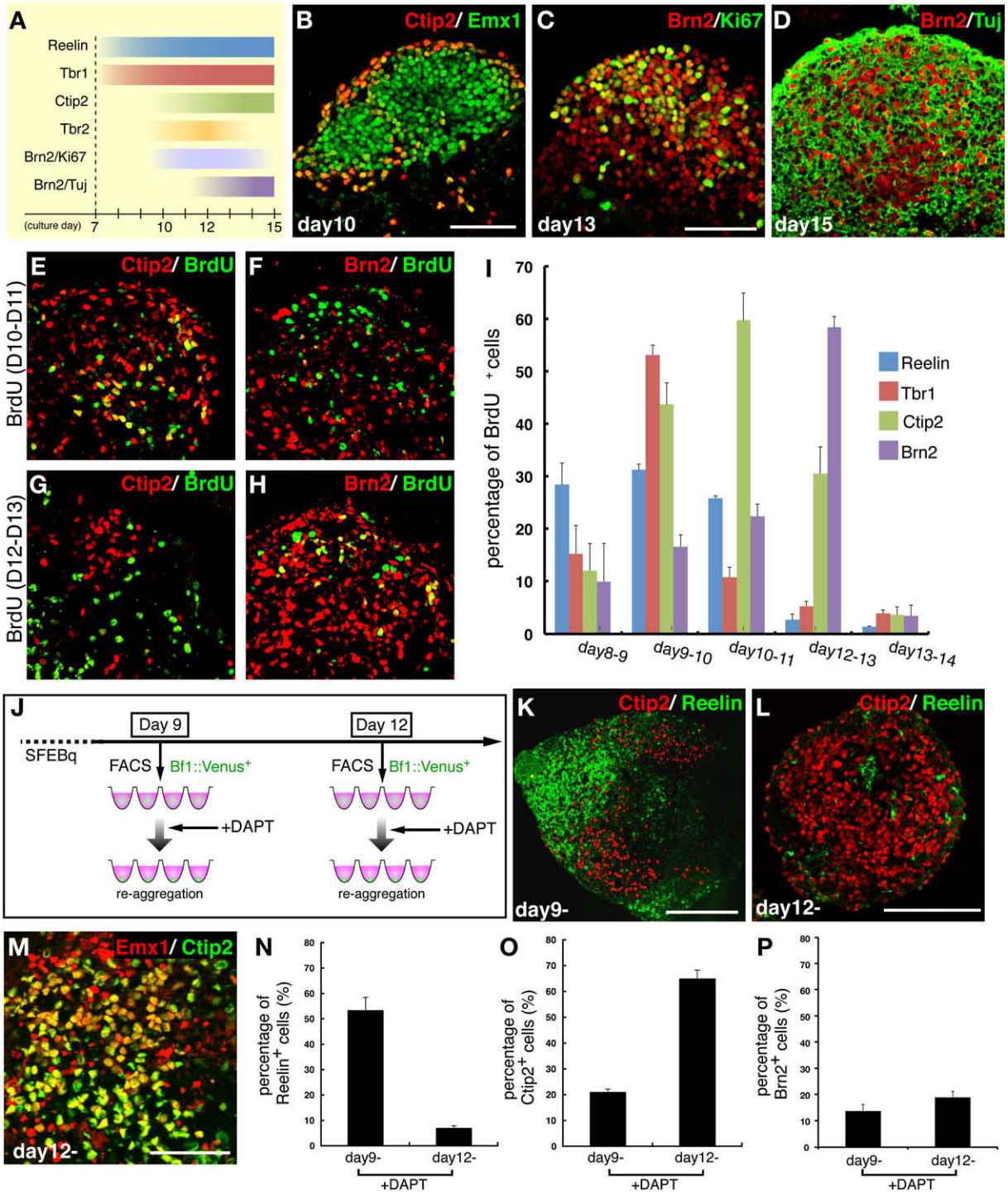

Figure 5. Layer-Specific Cortical Neurons Are Generated in the Temporally Controlled Manner that Mimics Corticogenesis In Vivo

(A) The expression onset of distinct cortical neuronal markers.

(B–D) Immunostaining of Citp2 and Emx1 on day 10 (B), Brn2 and Ki67 on day 13 (C) and Brn2 and Tuj1 on day 15 (D).

(E–I) Birth-date analysis using BrdU-pulse-labeling culture on the indicated days. Cryosections of SFEBq aggregates on day 16 were immunostained for BrdU (E–H), Ctip2 (E and G) and Brn2 (F and H) after overnight treatment with BrdU on day 10 (E and F) or day 12 (G and H). (I) Quantification of the BrdU$^+$ cells expressing each cell-type-specific marker.

(J) Schematic of the experiment of timed neuronal induction.

(K and L) Expression of Reelin and Ctip2 in the cultured aggregates after forced induction on day 9 (K) and day 12 (L).

(M) Ctip2$^+$ cells in the experiment of (L) were Emx1$^+$.

generation of patterned cortical neuroepithelial tissues from patternless ESC aggregates.

Such remarkable apical-basal arrangement is not observed in neurosphere culture (subjected to quick reaggregation into similarly-sized spheres), whether the cell source is dissociated mouse cortical tissues (E13–E15) or dissociated SFEBq-induced cortical cells (day 10) (data not shown). Therefore, a simple self-sorting mechanism (sorting via selective cell adhesion; Townes and Holtfreter, 1955) of different cortical components within the aggregate alone cannot fully explain the formation of this organized structure, suggesting that the continuous presence and function of polarized mitotic neuroepithelia are essential for this self-organization. Notch may provide one of the key signals that supports the maintenance of such neuroepithelia, give that, for instance, the disappearance of the rosette structures is accelerated by DAPT treatment during days 8–10 (Figures S1P and S1Q).

With respect to the neuroepithelial structures, there is an intriguing difference between the mESC- and hESC-derived cortical tissues. In the mESC-derived cortical tissues, the continuous neuroepithelia reform into several polarized circular neuroepithelia after day 7 of SFEBq culture (Figure 1G), and these rigid rosette structures gradually become less organized after day 12 as mitotic neuronal progenitors decrease. In contrast, the hESC-derived tissues retain a more continuous neuroepithelial structure even on day 46 (Figure 6). In some aggregates, a single (often folded) continuous neuropithelial structure occupies the most area in the aggregate even after such long-term culture (Figure S7E). One interpretation of this difference in structural stability is that the balance between differentiation and self-renewal may be different between hESC- and mESC-derived progenitors, in a manner that favors the hESC-derived neuroepithelia (note that the Pax6$^+$ mitotic zones in the day 46 human neuroepithelia are much thicker than the mouse ones on day 10; Figure 6). Another possible explanation is that hESC-derived neural progenitors generally have a greater mechanic tendency to form rigid epithelial structures, which may be relevant to the large size of the human cortex.

Prospective

As compared to previous approaches for ESC differentiation, the SFEBq culture is unique in that it supports the tissue formation of cortical neuroepithelia in a spatially and temporally controlled pattern, rather than just the differentiation of certain desired neurons. The in vitro generation of cortical tissues from ESCs by SFEBq culture will help elucidate various basic aspects of corticogenesis by providing a versatile in vitro system for studying complex events such as neocortical arealization, axonal guidance, and neuronal migration.

The in vitro generation of six-layered neocortical tissues is an intriguing but challenging task for future investigation. One of the major technical obstacles for this long-term goal is the current inability to form an inside-out pattern in SFEBq culture (Figure 6; day 16). The inside-out pattern is not observed in earlier rosettes, either, and our preliminary double-pulse labeling analyses using BrdU/IdU (day 8/9 or day 9/10) have shown that later-born neurons are not necessarily located in the relatively outer zone of the rosette on day 12 (Figure S6P) or day 13 (data not shown). Further mechanistic understanding of elementary regulatory factors is essential for a future success in the in vitro production of well-stratified cortical tissues, as well as major technical innovations enabling the long-term, three-dimensional culture of thick cortical tissues.

Nonetheless, the efficient and region/layer-specific generation of cortical tissues by the current SFEBq method should provide a valuable resource of functional cortical neurons and tissues for use in future medical applications. Since SFEBq-induced cortical tissues form self-organized long-range neuronal networks (Figures 2 and 3), they should be much more useful in determining pathogenesis, drug discovery and regenerative medicine for intractable brain diseases than isolated neurons are. Moreover, pathogenesis and drug discovery studies could be improved by combing the SFEBq culture with disease-specific human iPS cells (Takahashi et al., 2007), given that the SFEBq procedure with the ROCK inhibitor (used in this study for human ESCs) is also applicable to human iPS cell culture (see the Supplemental Experimental Procedures).

With respect to regenerative medicine, given that the SFEBq culture allows both Fgf8-induced rostral cortex specification (Figure 4) and enrichment of the layer-specific neurons (Figure 5), one attractive topic of future investigation is to finely direct the differentiation and selection of Ctip2$^+$ layer-V neurons of the motor cortex (part of the Coup-TF1$^-$ rostral cortex) from hESCs, which are lost in the ALS patient. In fact, Fgf8-treated SFEBq tissues (from mESCs) contain numerous Coup-TF1$^-$/Ctip2$^+$ layer-V neurons (Figures S4G–S4I). Detailed mechanistic understanding of neocortical arealization should be vital to promote this direction of application.

EXPERIMENTAL PROCEDURES

ESC Culture

Mouse ESCs (EB5) and Bf1::Venus ESCs (number 2-1) were maintained as described (Watanabe et al., 2005). Differentiation Medium was prepared as follows: G-MEM supplemented with 10% Knockout Serum Replacement (KSR; Invitrogen), 2 mM glutamine, 1 mM pyruvate, 0.1 mM nonessential amino acids, 0.1 mM 2-ME, 250 ng/ml recombinant human Dkk-1, and 1 μg/ml recombinant human Lefty-1 (which can be replaced by 10 μM SB431542). For SFEBq culture, ESCs were dissociated to single cells in 0.25% trypsin-EDTA (Invitrogen) and quickly reaggregated in differentiation medium (3000 cells/150 μl/well) using 96-well low cell-adhesion plates (Sumilon Spheroid Plates, Sumitomo; Lipidure-coat U96w from Nunc can also be used). On day 7, cell aggregates were transferred to a 10 cm bacterial-grade dish in N2 medium (DMEM/F12 supplemented with N2). The day on which ESCs were seeded to differentiate is defined as differentiation day 0.

hESCs were maintained and cultured as described (Watanabe et al., 2007). Differentiation Medium for SFEBq was the same with that for mESCs except that G-MEM/10% KSR is replaced with DMEM/F12/20% KSR for hESCs. Additional details are in the Supplemental Experimental Procedures.

Immunostaining, FACS Sorting, and Reaggregation Culture

Immunocytochemistry was performed as described (Watanabe et al., 2005, 2007) using antibodies listed in the Supplemental Experimental Procedures. Values shown on graphs represent the mean ± SE. For FACS analysis, cells

(N–P) The cell percentages of Reelin$^+$ (N), Ctip2$^+$ (O), and Brn2$^+$ (P).
Scale bars: 100 μm in (B), (C), and (D); 100 μm in (K) and (L); and 60 μm in (M). The bars in the graph represent standard errors.

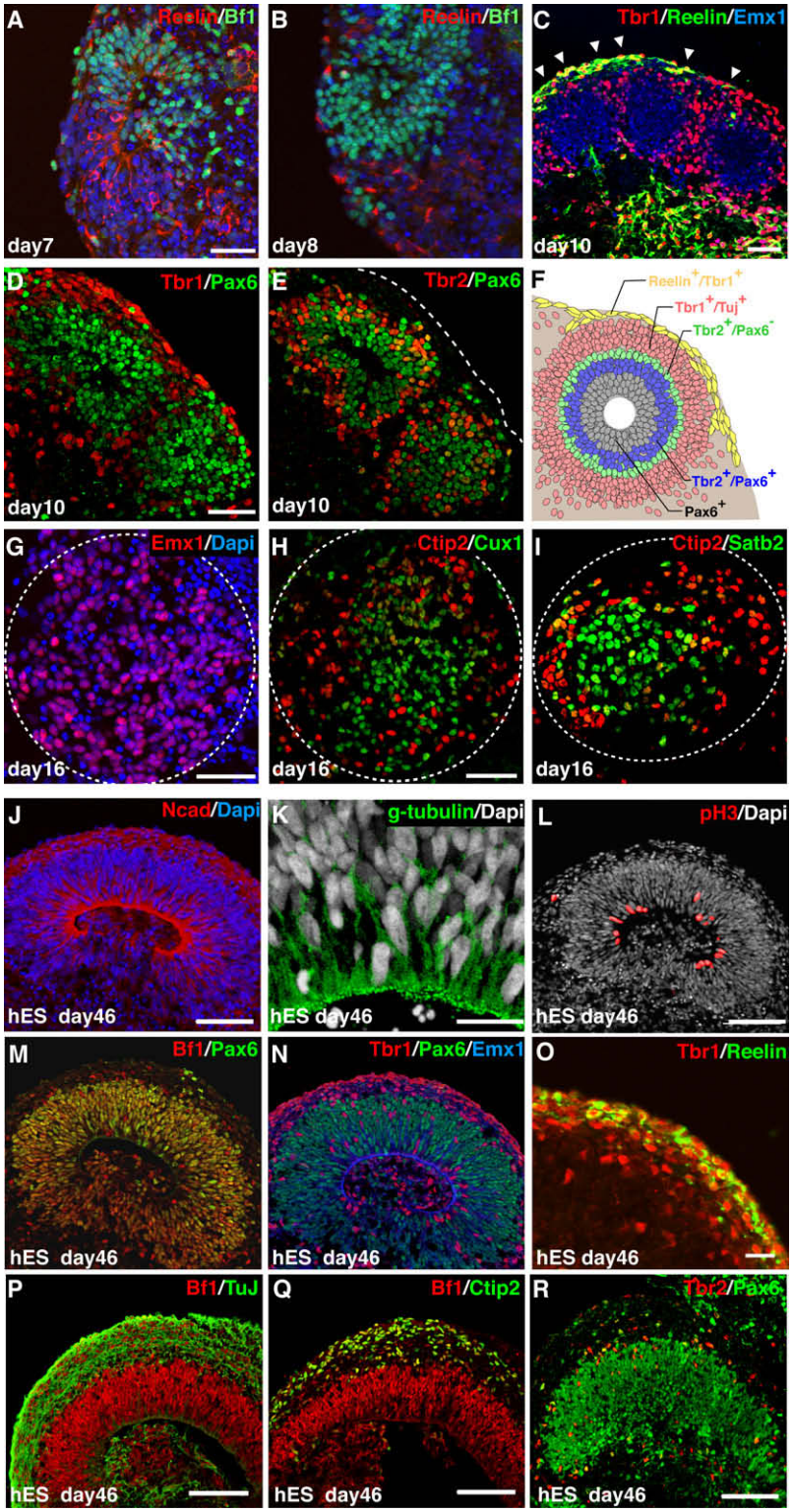

Figure 6. Self-Organized Formation of Polarized Cortical Tissues from SFEBq-Cultured mESCs

(A and B) Cryosections of SFEBq-cultured mESC aggregates on day 7 (A) and day 8 (B) were immunostained with Reelin and Bf1.

(C) Reelin$^+$/Tbr1$^+$ neurons and Emx1$^+$ rosettes on day 10. Arrowheads, Reelin$^+$/Tbr1$^+$ neurons in the superficial zone (facing to the aggregate surface) of the Emx1$^+$ rosettes.

(D and E) Immunostaining of the cortical markers Pax6, Tbr1 (D), and Tbr2 (E) on day 10.

(F) Schematic of the cellular distribution pattern of the SFEBq-induced cortical rosette.

(G–I) The distribution of the early/lower CP marker Ctip2 (H and I) and the late/upper CP marker Cux1 (H) and Satb2 (I) in Emx1$^+$ clusters (G).

(J–R) Cryosections of SFEBq-cultured hESC aggregates on day 46 were stained for cortical markers, as indicated in each panel. In (J) and (L)–(N), confocal images of serial sections at the same region are shown. (K) shows a high power image of the perilumenal portion. The hESC-derived Bf1$^+$/N-cadherin$^+$ neuroepithelial structure coexpressed Pax6 (M) and Emx1 (N). Tbr1 (N) and Ctip2 (Q) were expressed in the TuJ1$^+$ zone located superficially to the Bf1$^+$/Pax6$^+$ neuroepithelium, while Tbr2$^+$ cells were mostly found in or adjacent to the Pax6$^+$ neuroepithelial zone.

Scale bars: 30 μm in (A) and (B); 50 μm in (C), (D), and (E); 60 μm in (G)–(I); 20 μm in (K); and 100 μm in (J), (L)–(O), (P), and (R).

were counted with FACSAria (BD), and the data were analyzed with the FACSDiva software (BD). The sorted cells were collected in ice-cold N2 medium containing 10% FBS and quickly reaggregated using low cell-adhesion 96-well culture plates (5000 cells/well). Recombinant mouse FGF8b (50 ng/ml), mouse FGFR3-fc (500 ng/ml), human BMP4 (0.5 ng/ml), and human Wnt3a (20 ng/ml) were added to the culture medium. For forced neuronal differentiation, DAPT (10 μM) was added on the next day of FACS sorting. For induction of Tbx21$^+$ neurons, Bf1::Venus$^+$ cells were sorted by FACS and reaggregated on day 7, treated with FGF8 (50 ng/ml), and DAPT (10 μM) from day 8 and cultured for 2 weeks. Tbx21$^+$ neurons were not induced by DAPT treatment alone.

Birth-Date Analysis

For in vitro birth-date analysis (Ajioka and Nakajima, 2005), aggregates were treated with BrdU (5 μg/ml) on day 8, 9, 10, 12, or 14 and rinsed with medium to remove it on the next day. On day 16, cell aggregates were fixed and cryosectioned. Sections were immunostained for BrdU and each layer-specific marker as indicated in Figure 5. The percentages of BrdU$^+$ cells in the Bf1$^+$/Ctip2$^+$ (most of the Ctip2$^+$ cells were Emx1$^+$), Bf1$^+$/Brn2$^+$, Reelin$^+$, or Tbr1$^+$ cells were quantified. For the quantification, 20–25 aggregates were examined for each experiment, which was repeated at least three times.

Brain Slice Coculture Assay

For coculture with forebrain slices, E14.5 or P1 mouse brains were excised, and coronal sections (200 μm) were prepared using a vibratome (F1000SL, Leica). Bf1::Venus$^+$ neuronal masses were cut out in appropriate sizes from the SFEBq cell aggregates under a fluorescent dissecting microscope and cocultured with the forebrain slice (by inserting the masses into the ventricle space so that the inserted aggregates were in contact with both pallial and subpallial walls) for 3 or 6 days on a Transwell culture insert (Corning) containing the slice-culture medium (DMEM/F12, N2 supplement, 15% FBS, and penicillin-streptomycin) under 40% O_2 and 5% CO_2 conditions.

Ca^{2+} Imaging

For Ca^{2+} imaging, cell aggregates were subjected to filter culture using a Transwell culture insert (Corning) in the N2 medium on day 18. On day 21 or 24, the aggregate was incubated in fluo4-AM solution as described previously (Ikegaya et al., 2005). Additional details are in the Supplemental Experimental Procedures.

SUPPLEMENTAL DATA

The Supplemental Data include Supplemental Experimental Procedures, seven figures, and four movies and can be found with this article online at http://www.cellstemcell.com/supplemental/S1934-5909(08)00455-4.

ACKNOWLEDGMENTS

We are grateful to Drs. H. Enomoto and C. Hanashima for invaluable comments, to Dr. A. Miyawaki for *Venus* cDNA, to Dr. Y. Yoshihara for Tbx21 antibody, to Dr. Y. Ono for Lmx1a antibody, to Dr. K. Mori for Telencephalin antibody, to Dr. M. Ikeya for advice on homologous recombination, and to members of the Sasai lab for discussion and advice. This work was supported by grants-in-aid from MEXT, the Kobe Cluster Project, and the Leading Project (Y.S.).

Received: July 31, 2008
Revised: September 6, 2008
Accepted: September 9, 2008
Published: November 5, 2008

REFERENCES

Adelsberger, H., Garaschuk, O., and Konnerth, A. (2005). Cortical calcium waves in resting newborn mice. Nat. Neurosci. *8*, 988–990.

Ajioka, I., and Nakajima, K. (2005). Birth-date-dependent segregation of the mouse cerebral cortical neurons in reaggregation cultures. Eur. J. Neurosci. *22*, 331–342.

Arlotta, P., Molyneaux, B.J., Chen, J., Inoue, J., Kominami, R., and Macklis, J.D. (2005). Neuronal subtype-specific genes that control corticospinal motor neuron development in vivo. Neuron *45*, 207–221.

Bielle, F., Griveau, A., Narboux-Neme, N., Vigneau, S., Sigrist, M., Arber, S., Wassef, M., and Pierani, A. (2005). Multiple origins of Cajal-Retzius cells at the borders of the developing pallium. Nat. Neurosci. *8*, 1002–1012.

Englund, C., Fink, A., Lau, C., Pham, D., Daza, R.A., Bulfone, A., Kowalczyk, T., and Hevner, R.F. (2005). Pax6, Tbr2, and Tbr1 are expressed sequentially by radial glia, intermediate progenitor cells, and postmitotic neurons in developing neocortex. J. Neurosci. *25*, 247–251.

Frantz, G.D., and McConnell, S.K. (1996). Restriction of late cerebral cortical progenitors to an upper-layer fate. Neuron *17*, 55–61.

Garaschuk, O., Linn, J., Eilers, J., and Konnerth, A. (2000). Large-scale oscillatory calcium waves in the immature cortex. Nat. Neurosci. *3*, 452–459.

Gaspard, N., Bouschet, T., Hourez, R., Dimidschstein, J., Naeije, G., van den Ameele, J., Espuny-Camacho, I., Herpoel, A., Passante, L., Schiffmann, S.N., et al. (2008). An intrinsic mechanism of corticogenesis from embryonic stem cells. Nature *455*, 355–357.

Gonzalez, J.L., Russo, C.J., Goldowitz, D., Sweet, H.O., Davisson, M.T., and Walsh, C.A. (1997). Birthdate and cell marker analysis of scrambler: a novel mutation affecting cortical development with a reeler-like phenotype. J. Neurosci. *17*, 9204–9211.

Guillemot, F. (2005). Cellular and molecular control of neurogenesis in the mammalian telencephalon. Curr. Opin. Cell Biol. *17*, 639–647.

Hanashima, C., Li, S.C., Shen, L., Lai, E., and Fishell, G. (2004). Foxg1 suppresses early cortical cell fate. Science *303*, 56–59.

Hebert, J.M., Hayhurst, M., Marks, M.E., Kulessa, H., Hogan, B.L., and McConnell, S.K. (2003a). BMP ligands act redundantly to pattern the dorsal telencephalic midline. Genesis *35*, 214–219.

Hebert, J.M., Lin, M., Partanen, J., Rossant, J., and McConnell, S.K. (2003b). FGF signaling through FGFR1 is required for olfactory bulb morphogenesis. Development *130*, 1101–1111.

Hevner, R.F., Daza, R.A., Rubenstein, J.L., Stunnenberg, H., Olavarria, J.F., and Englund, C. (2003a). Beyond laminar fate: toward a molecular classification of cortical projection/pyramidal neurons. Dev. Neurosci. *25*, 139–151.

Hevner, R.F., Neogi, T., Englund, C., Daza, R.A., and Fink, A. (2003b). Cajal-Retzius cells in the mouse: transcription factors, neurotransmitters, and birthdays suggest a pallial origin. Brain Res. Dev. Brain Res. *141*, 39–53.

Hevner, R.F., Shi, L., Justice, N., Hsueh, Y., Sheng, M., Smiga, S., Bulfone, A., Goffinet, A.M., Campagnoni, A.T., and Rubenstein, J.L. (2001). Tbr1 regulates differentiation of the preplate and layer 6. Neuron *29*, 353–366.

Ikegaya, Y., Le Bon-Jego, M., and Yuste, R. (2005). Large-scale imaging of cortical network activity with calcium indicators. Neurosci. Res. *52*, 132–138.

Kinney, J.W., Davis, C.N., Tabarean, I., Conti, B., Bartfai, T., and Behrens, M.M. (2006). A specific role for NR2A-containing NMDA receptors in the maintenance of parvalbumin and GAD67 immunoreactivity in cultured interneurons. J. Neurosci. *26*, 1604–1615.

Lee, S.M., Tole, S., Grove, E., and McMahon, A.P. (2000). A local Wnt-3a signal is required for development of the mammalian hippocampus. Development *127*, 457–467.

Mangale, V.S., Hirokawa, K.E., Satyaki, P.R., Gokulchandran, N., Chikbire, S., Subramanian, L., Shetty, A.S., Martynoga, B., Paul, J., Mai, M.V., et al. (2008). Lhx2 selector activity specifies cortical identity and suppresses hippocampal organizer fate. Science *319*, 304–309.

Mitsui, S., Saito, M., Mori, K., and Yoshihara, Y. (2007). A transcriptional enhancer that directs telencephalon-specific transgene expression in mouse brain. Cereb. Cortex *17*, 522–530.

Molyneaux, B.J., Arlotta, P., Menezes, J.R., and Macklis, J.D. (2007). Neuronal subtype specification in the cerebral cortex. Nat. Rev. Neurosci. *8*, 427–437.

Monuki, E.S., and Walsh, C.A. (2001). Mechanisms of cerebral cortical patterning in mice and humans. Nat. Neurosci. *4* (*Suppl*), 1199–1206.

Nagai, T., Ibata, K., Park, E.S., Kubota, M., Mikoshiba, K., and Miyawaki, A. (2002). A variant of yellow fluorescent protein with fast and efficient maturation for cell-biological applications. Nat. Biotechnol. *20*, 87–90.

Nelson, B.R., Hartman, B.H., Georgi, S.A., Lan, M.S., and Reh, T.A. (2007). Transient inactivation of Notch signaling synchronizes differentiation of neural progenitor cells. Dev. Biol. *304*, 479–498.

O'Leary, D.D., Chou, S.J., and Sahara, S. (2007). Area patterning of the mammalian cortex. Neuron *56*, 252–269.

Puelles, L., Kuwana, E., Puelles, E., Bulfone, A., Shimamura, K., Keleher, J., Smiga, S., and Rubenstein, J.L. (2000). Pallial and subpallial derivatives in the embryonic chick and mouse telencephalon, traced by the expression of the genes Dlx-2, Emx-1, Nkx-2.1, Pax-6, and Tbr-1. J. Comp. Neurol. *424*, 409–438.

Rallu, M., Corbin, J.G., and Fishell, G. (2002). Parsing the prosencephalon. Nat. Rev. Neurosci. *3*, 943–951.

Shen, Q., Wang, Y., Dimos, J.T., Fasano, C.A., Phoenix, T.N., Lemischka, I.R., Ivanova, N.B., Stifani, S., Morrisey, E.E., and Temple, S. (2006). The timing of cortical neurogenesis is encoded within lineages of individual progenitor cells. Nat. Neurosci. *9*, 743–751.

Shimogori, T., and Grove, E.A. (2005). Fibroblast growth factor 8 regulates neocortical guidance of area-specific thalamic innervation. J. Neurosci. *25*, 6550–6560.

Soriano, E., and Del Rio, J.A. (2005). The cells of cajal-retzius: still a mystery one century after. Neuron *46*, 389–394.

Stoykova, A., Hatano, O., Gruss, P., and Gotz, M. (2003). Increase in reelin-positive cells in the marginal zone of Pax6 mutant mouse cortex. Cereb. Cortex *13*, 560–571.

Takahashi, K., Tanabe, K., Ohnuki, M., Narita, M., Ichisaka, T., Tomoda, K., and Yamanaka, S. (2007). Induction of pluripotent stem cells from adult human fibroblast by defined factors. Cell *131*, 861–872.

Tao, W., and Lai, E. (1992). Telencephalon-restricted expression of BF-1, a new member of the HNF-3/fork head gene family, in the developing rat brain. Neuron *8*, 957–966.

Townes, P., and Holtfreter, J. (1955). Directed movement and selective adhesion of embryonic amphibian. J. Exp. Zool. *128*, 53–120.

Watanabe, K., Kamiya, D., Nishiyama, A., Katayama, T., Nozaki, S., Kawasaki, H., Watanabe, Y., Mizuseki, K., and Sasai, Y. (2005). Directed differentiation of telencephalic precursors from embryonic stem cells. Nat. Neurosci. *8*, 288–296.

Watanabe, K., Ueno, M., Kamiya, D., Nishiyama, A., Matsumura, M., Wataya, T., Takahashi, J.B., Nishikawa, S., Muguruma, K., and Sasai, Y. (2007). A ROCK inhibitor permits survival of dissociated human embryonic stem cells. Nat. Biotechnol. *25*, 681–686.

Wataya, T., Ando, S., Muguruma, K., Ikeda, H., Watanabe, K., Eiraku, M., Kawada, M., Takahashi, J., Hashimoto, N., and Sasai, Y. (2008). Minimization of Exogenous Signals in ES Cell Culture Induces Rostral Hypothalamic Differentiation. Proc. Natl. Acad. Sci. USA *105*, 11796–11801.

Weigmann, A., Corbeil, D., Hellwig, A., and Huttner, W.B. (1997). Prominin, a novel microvilli-specific polytopic membrane protein of the apical surface of epithelial cells, is targeted to plasmalemmal protrusions of non-epithelial cells. Proc. Natl. Acad. Sci. USA *94*, 12425–12430.

Yoshihara, S., Omichi, K., Yanazawa, M., Kitamura, K., and Yoshihara, Y. (2005). Arx homeobox gene is essential for development of mouse olfactory system. Development *132*, 751–762.

Yuste, R., Nelson, D.A., Rubin, W.W., and Katz, L.C. (1995). Neuronal domains in developing neocortex: mechanisms of coactivation. Neuron *14*, 7–17.

Zhou, C., Tsai, S.Y., and Tsai, M.J. (2001). COUP-TFI: an intrinsic factor for early regionalization of the neocortex. Genes Dev. *15*, 2054–2059.